*Inorg. Chem.* **2008**, *47*, 2380−2388

# Refining the Active Site Structure of Iron−Iron Hydrogenase Using Computational Infrared Spectroscopy

**Jesse W. Tye**, **Marcetta Y. Darensbourg**, **and Michael B. Hall***

*Department of Chemistry, Texas A&M University, College Station, Texas 77843-3255*

Received July 10, 2007

Iron−iron hydrogenases ([FeFe]$H_2$ases) are exceptional natural catalysts for the reduction of protons to dihydrogen. Future biotechnological applications based on these enzymes require a precise understanding of their structures and properties. Although the [FeFe]$H_2$ases have been characterized by single-crystal X-ray crystallography and a range of spectroscopic techniques, ambiguities remain regarding the details of the molecular structures of the spectroscopically observed forms. We use density functional theory (DFT) computations on small-molecule computational models of the [FeFe]$H_2$ase active site to address this problem. Specifically, a series of structural candidates are geometry optimized and their infrared (IR) spectra are simulated using the computed C−O and C−N stretching frequencies and infrared intensities. Structural assignments are made by comparing these spectra to the experimentally determined IR spectra for each form. The $H_{red}$ form is assigned as a mixture of an $Fe^IFe^I$ form with an open site on the distal iron center and either a $Fe^IFe^I$ form in which the distal cyanide has been protonated or a $Fe^{II}Fe^{II}$ form with a bridging hydride ligand. The $H_{ox}$ form is assigned as a valence-localized $Fe^IFe^{II}$ redox level with an open site at the distal iron. The $H_{ox}^{air}$ form is assigned as an $Fe^{II}Fe^{II}$ redox level with $OH^-$ or $OOH^-$ bound to the distal iron center that may or may not have an oxygen atom bound to one of the sulfur atoms of the dithiolate linker. Comparisons of the computed IR spectra of the $^{12}CO$ and $^{13}CO$ inhibited form with the experimental IR spectra show that exogenous CO binds terminally to the distal iron center.

## Introduction

Hydrogenase enzymes are used by certain microorganisms in nature to facilitate the reversible oxidation of dihydrogen to protons and electrons, $H_2 \leftrightarrow 2H^+ + 2e^-$.[1–3] Although a particular enzyme in an organism is generally dedicated to either $H_2$ production or $H_2$ consumption in vivo, the reaction can be driven in either direction in vitro by supplying either $H_2$ pressure or $H^+$ and $e^-$ under appropriate conditions. The functional and structural properties of these enzymes are of considerable interest because of their potential uses in biotechnological applications such as hydrogen fuel cells. In fact, the [NiFe] hydrogenase enzyme from *Allochromatium vinosum* has been shown to function as an excellent heterogeneous catalyst for $H_2$ oxidation when absorbed onto a graphite electrode.[4–7] This enzyme-modified electrode was shown to oxidize dihydrogen at oxidation potentials and $H_2$ pressures that rival platinum metal.[4]

Hydrogenase enzymes can be classified into [NiFe][8] and [FeFe][11,12] based on the metal content of their active sites. Among these enzymes, the [NiFe] hydrogenases are mostly found in hydrogen-oxidizing enzymes, while the [FeFe] hydrogenases are mostly found in hydrogen-producing

* To whom correspondence should be addressed. E-mail: marcetta@mail.chem.tamu.edu (M.Y.D.), mbhall@tamu.edu (M.B.H.).

(1) Adams, M. W. W. *Biochim. Biophys. Acta* **1990**, *1020*, 115–145.
(2) Albracht, S. P. J. *Biochim. Biophys. Acta* **1994**, *1188*, 167–204.
(3) Frey, M. *Structure and Bonding*; Springer-Verlag: Berlin, Heidelberg, 1998; Vol. *90*, pp 98–126.
(4) Lamle, S. E.; Vincent, K. A.; Halliwell, L. M.; Albracht, S. P. J.; Armstrong, F. A. *Dalton Trans.*, **2003**, *21*, 4152–4157.
(5) Mertens, R.; Liese, A. *Curr. Opin. Biotech.* **2004**, *15*, 343–348.
(6) Vincent, K. A.; Cracknell, J. A.; Lenz, O.; Zebger, I.; Friedrich, B.; Armstrong, F. A. *Proc. Natl. Acad. Sci. U. S. A.* **2005**, *102*, 16951–16954.
(7) Tye, J. W.; Hall, M. B.; Darensbourg, M. Y. *Proc. Natl. Acad. Sci. U. S. A.* **2005**, *102*, 16911–16912.
(8) Przybyla, A. E.; Robbins, J.; Menon, N.; Peck, H. D., Jr. *FEMS Microbiol. Rev.* **1992**, *8*, 109–135.
(9) Garcin, E.; Vernede, X.; Hatchikian, E. C.; Volbeda, A.; Frey, M.; Fontecilla-Camps, J. C. *Structure* **1999**, *7*, 557–566.
(10) Teixeira, M.; Moura, I.; Xavier, A. V.; Huynh, B. H.; Der Vartanian, D. V.; Peck, H. D.; LeGall, J.; Moura, J. J. G. *J. Biol. Chem.* **1985**, *260*, 8942–8950.
(11) Nicolet, Y.; Lemon, B. J.; Fontecilla-Camps, J. C.; Peters, J. W. *Trends Biochem. Sci.* **2000**, *25*, 138–143.
(12) Peters, J. W. *Curr. Opin. Struct. Biol.* **1999**, *9*, 670–676.



10.1021/ic7013732 CCC: $40.75 
Published on Web 02/28/2008

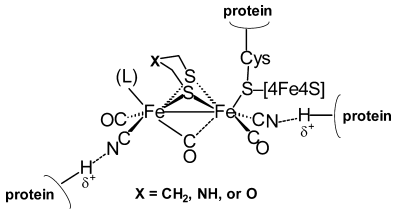


**Figure 1.** Structure of the active site of [FeFe]H$_2$ases. The two iron centers are commonly designated by their spatial relation to the [4Fe4S] cluster and, thus, are referred to as the distal iron (left) and proximal iron (right). The nature of the L ligand and the "bridging" CO ligand (fully bridging vs semibridging vs terminal to the distal iron) apparently depends on the redox state of the FeFe cluster.

enzymes. Although the [NiFe] enzymes are generally considered more thermally and $O_2$ stable, the [FeFe] enzyme active site has proven more amenable to synthetic model studies due to its resemblance to the well-known organometallic complex ($\mu$-pdt)[Fe(CO)$_3$]$_2$ (pdt = propanedithiolate = $-S(CH_2)_3S-$).[13,14]

The [FeFe] hydrogenase enzymes derived from two different organisms have been studied by single crystal X-ray diffraction, yielding four different structures. These two enzymes have many structural similarities in spite of their different sources and crystallization conditions.[11,12] The molecular structures of both enzymes feature an unusual 6-Fe active site cluster (the so-called H-cluster) and two or more ferrodoxin type Fe−S clusters, which connect the H cluster to the enzyme surface.

The H-cluster (Figure 1) is the putative site of $H^+$ reduction and $H_2$ oxidation, and consists of an unusual di-iron cluster bridged to a typical [4Fe−4S] cluster by a protein-bound cysteinate ligand.[11,15–18] Each iron atom of the di-iron cluster is further coordinated by one terminally bound CN and one terminally bound CO ligand. The two irons are bridged by a novel five-atom cofactor generally assigned as either 1,3-propanedithiolate (pdt, $-SCH_2CH_2CH_2S-$)[11] or 1,3-di(thiomethyl)amine (DTMA, $-SCH_2NHCH_2S-$).[18] A third CO ligand either is found to bridge the two irons atoms or is terminally bound to the distal iron atom, depending on the redox state of the di-iron cluster. Incubation of the catalytically active $H_{ox}$ form of the enzyme with CO gas results in a catalytically inactive, CO-inhibited form of the enzyme.[16]

Mössbauer,[19–21] electron paramagnetic resonance (EPR),[22–26] and infrared (IR) spectral studies[18,27–30] have identified three redox states of the di-iron cluster, while the [4Fe−4S] portion of the H-cluster apparently remains in the EPR-silent [4Fe−4S]$^{2+}$ redox state. The aerobic purification of the enzyme results in an "overoxidized", catalytically inactive redox state (labeled as $H_{as\text{-}isolated}$ or $H_{ox}^{air}$), which is EPR-silent. Electrochemical reduction or the incubation of the inactive enzyme with $H_2$ leads to a second EPR-silent, two-electron reduced species, labeled as $H_{red}$. The oxidation of the $H_{red}$ form, either electrochemically or by auto-oxidation via $H_2$ loss, leads to a catalytically active, paramagnetic ($S = {}^1/_2$) form, labeled as $H_{ox}$. Recently, Parkin et al. prepared an anaerobically overoxidized state of the enzyme.[31] This overoxidized state is itself catalytically inactive for $H_2$ oxidation or $H^+$ reduction but is more quickly reactivated by application of a reducing current than $H_{ox}^{air}$.

Synthetic model studies[14] suggested that the $H_{ox}^{air}$, $H_{ox}$, and $H_{red}$ forms correspond respectively to $Fe^{II}Fe^{II}$, $Fe^{I}Fe^{II}$, and $Fe^{I}Fe^{I}$ formal redox states of the 2-Fe cluster. Density functional theory calculations have been applied by several research groups to give a better understanding of the molecular details of $H_2$ oxidation and $H^+$ reduction at the di-iron active site. In an early computational study on this system, Cao and Hall[32] were able to confirm the proposed oxidation state assignments ($Fe^{II}$ to $Fe^{I}$) and suggested a mechanism in which $H_2$ is bound to the terminal site of the distal iron and heterolytically cleaved to produce a terminally bound hydride species. Fiedler and Brunold showed that inclusion of the neighboring [4Fe−4S] is important for proper modeling of the EPR parameters of the $H_{ox}$ and $H_{ox}$−CO forms.[33] Fan and Hall[34] established that a bridgehead amine provides a kinetically and thermodynamically favorable route for the proton transfer in the heterolytic cleavage of $H_2$. Liu and Hu[35,36] came to the same conclusion in a subsequent study. Cao and Hall also reported that an $Fe^{II}Fe^{II}$ complex with a bridging hydride ligand and all terminal CO ligands was more stable than the constitutional isomer with a bridging CO ligand

(13) Seyferth, D.; Womack, G. B.; Gallagher, M. K.; Cowie, M.; Hames, B. W.; Fackler, J. P., Jr.; Mazany, A. M *Organometallics* **1987**, *6*, 283–294.
(14) (a) Lyon, E. J.; Georgakaki, I. P.; Reibenspies, J. H.; Darensbourg, M. Y. *Angew. Chem., Int. Ed.* **1999**, *38*, 3178–3180. (b) Le Cloirec, A.; Davies, S. C.; Evans, D. J.; Hughes, D. L.; Pickett, C. J.; Best, S. P.; Borg, S. *Chem. Commun.* **1999**, 2285–2286. (c) Schmidt, M.; Contakes, S. M.; Rauchfuss, T. B. *J. Am. Chem. Soc.* **1999**, *121*, 9736–9737.
(15) Peters, J. W.; Lanzilotta, W. N.; Lemon, B. J.; Seefedt, L. C. *Science* **1998**, *282*, 1853–1858.
(16) Lemon, B. J.; Peters, J. W. *Biochemistry* **1999**, *39*, 12969–12973.
(17) Nicolet, Y.; Piras, C.; Legrand, P.; Hatchikian, C. E.; Fontecilla-Camps, J. C. *Structure* **1999**, *7*, 13–23.
(18) Nicolet, Y.; De Lacey, A. L.; Vernede, X.; Fernandez, V. M.; Hatchikian, E. C.; Fontecilla-Camps, J. C. *J. Am. Chem. Soc.* **2001**, *123*, 1596–1601.
(19) Rusnak, F. M.; Adams, M. W. W.; Mortenson, L. E.; Munck, E. *J. Biol. Chem.* **1987**, *262*, 38–41.
(20) Popescu, C. V.; Munck, E. *J. Am. Chem. Soc.* **1999**, *121*, 7877–7884.
(21) Pereira, A. S.; Tavares, P.; Moura, I.; Moura, J. J. G.; Huynh, B. H. *J. Am. Chem. Soc.* **2001**, *123*, 2771–2782.
(22) Adams, M. W. W.; Mortenson, L. E. *J. Biol. Chem.* **1984**, *259*, 7045–7055.
(23) Adams, M. W. W. *J. Biol. Chem.* **1987**, *262*, 15054–15061.
(24) Zambrano, I. C.; Kowal, A. T.; Mortenson, L. E.; Adams, M. W. W.; Johnson, M. K. *J. Biol. Chem.* **1989**, *264*, 20974–20983.
(25) Bennett, B.; Lemon, B. J.; Peters, J. W. *Biochemistry* **2000**, *39*, 7455–7560.
(26) Albracht, S. P. J.; Roseboom, W.; Hatchikian, E. C. J. *Biol Inorg. Chem.* **2006**, *11*, 88–101.
(27) Pierik, A. T.; Hulstein, M.; Hagen, W. R.; Albracht, S. P. J. *Eur. J. Biochem.* **1998**, *258*, 572–578.
(28) De Lacey, A. L.; Stadler, C.; Cavazza, C.; Hatchikian, E. C.; Fernandez, V. M. *J. Am. Chem. Soc.* **2000**, *122*, 11232–11233.
(29) Chen, Z.; Lemon, B. J.; Huang, S.; Swartz, D. J.; Peters, J. W.; Bagley, K. A. *Biochemistry* **2002**, *41*, 2036–2043.
(30) Roseboom, W.; Lacey, A. L.; Fernandez, V. M.; Hatchikian, E. C.; Albracht, S. P. J. *JBIC, J. Biol. Inorg. Chem.* **2006**, *11*, 102–118.
(31) Parkin, A.; Cavazza, C.; Fontecilla-Camps, J. C.; Armstrong, F. A. *J. Am. Chem. Soc.* **2006**, *128*, 16808.
(32) Cao, Z.; Hall, M. B. *J. Am. Chem. Soc.* **2001**, *123*, 3734–3742.
(33) Fiedler, A. T.; Brunold, T. C. *Inorg. Chem.* **2005**, *44*, 9322–9334.
(34) Fan, H.-J.; Hall, M. B. *J. Am. Chem. Soc.* **2001**, *123*, 3828–3829.
(35) Liu, Z-P.; Hu, P. *J. Am. Chem. Soc.* **2002**, *124*, 5175–5182.
(36) Liu, Z.-P.; Hu, P. *J. Chem. Phys.* **2002**, *117*, 8177–8180.

and a terminal hydride ligand.[32] De Gioia[37,38] and Zhou[39,40] and their respective co-workers have developed an alternative kinetically and thermodynamically favorable route for the heterolytic cleavage of bound $H_2$ based on this bridging hydride isomer and an active site rearrangement to create an open site between the two iron centers. In their mechanisms, dihydrogen binds to the proximal iron in the area "between" the two iron atoms and a proton is transferred from the bound $\eta^2$-$H_2$ to a $\mu$-S atom of the dithiolate bridge. A subsequent study by De Gioia and co-workers shows that protonation of a terminal hydride at the distal iron center leads to slightly lower barriers for $H_2$ formation than protonation of a bridging hydride ligand.[41]

The theoretical studies published to date utilize simple models of the first coordination sphere of the enzyme active site and thus do not include any of the surrounding protein residues. In order to produce a more accurate spectroscopic model, we have modeled three nearby residues that are hydrogen-bond donors to the [FeFe]$H_2$ase active site. In this way, we seek to identify and to characterize structural candidates for the spectroscopically observed $H_{red}$, $H_{ox}$, $H_{ox}$−CO, and $H_{ox}^{air}$ forms of the [FeFe]$H_2$ase enzyme.

### Computational Details

The effect of the local protein environment on the [FeFe]$H_2$ase active site was modeled by partial geometry optimizations in which simplified models of nearby amino acid side chains were frozen at their crystallographically determined positions about the enzyme active site (PDB code 1C4A[16]). The cysteine(C503)-[4Fe4S] unit was modeled as MeSH, and this S atom was frozen throughout the optimizations. Nearby cysteine, serine, and lysine amino acid residues (C299, S232, and K358 in 1C4A) were modeled as $CH_3SH$, $CH_3OH$, and $CH_3NH_2$, respectively, and the S, O, N, and C atoms were frozen at their crystallographically determined positions.

All DFT calculations were performed using a hybrid functional [the three-parameter exchange functional of Becke (B3)[42] and the correlation functional of Lee, Yang, and Parr (LYP)[43]] (B3LYP) as implemented in Gaussian 03.[44] The iron and sulfur atoms use the effective core potential and associated basis set of Hay and Wadt (LANL2DZ).[45,46] For iron, the two outermost p functions were replaced by reoptimized 4p functions as suggested by Couty and Hall[47] and an f polarization function[48] was added. For sulfur and phosphorus, the basis set was augmented by the d polarization function of Höllwarth et al.[49] The CO, CN, $H_2O$, H, and $H_2$ ligands, the OH and $NH_2$ of $CH_3OH$ and $CH_3NH_2$, the H attached to S in $CH_3SH$, and the central NH group of the DTMA bridge use the 6-31G(d′,p′) basis set.[50–52] All other atoms use the 6-31G basis set.[53] Unless otherwise noted, all geometries are fully optimized and confirmed as minima or $n$-order saddle points by analytical frequency calculations at the same level.

The DFT frequency calculations yield values for the energy (in $cm^{-1}$) and IR intensity of each $\nu$(CX) stretching mode. The absolute intensity and width of the IR bands is not determined by the DFT calculation, and experimentally, they are based on a number of factors, such as concentration, solvent, and counterions for charged species. The calculated $\nu$(CX) spectra are simulated using Gaussian functions with a full width at half-height (fwhh) of 10 $cm^{-1}$.

## Results and Discussion

**Experimental IR Spectra.** IR spectroscopy is a powerful tool for studying the [FeFe]$H_2$ase active site, as the metal-bound CO ligands are sensitive indicators of the geometry about and electron density at metal centers.[54] A list of experimentally determined $\nu$(CO) and $\nu$(CN) stretching frequencies for various forms of [FeFe]$H_2$ase enzymes derived from *Desulfovibrio desulfuricans* Hildenborough (DdH), *Desulfovibrio vulgaris* (Dv), and *Clostridium pasteurianum* I (CpI) are given in Table 1. Since the IR spectra of the [FeFe]$H_2$ase enzymes derived from DdH and Dv are nearly identical ($\pm$1 $cm^{-1}$) and DNA sequencing shows that these enzymes have the same amino acid sequence,[17] the results for DdH and Dv are reported together. For a given form of the enzyme, the values of the $\nu$(CO) and $\nu$(CN) bands are similar regardless of whether the enzyme was derived from DdH/Dv or CpI.

**Calibration of Computed $\nu_{CO}$ and $\nu_{CN}$ Values.** Density functional theory calculations with the B3LYP functional


(37) Bruschi, M.; Fantucci, P.; De Gioia, L. *Inorg. Chem.* **2002**, *41*, 1421–1429.
(38) Bruschi, M.; Fantucci, P.; De Gioia, L. *Inorg. Chem.* **2003**, *42*, 4773–4781.
(39) Zhou, T.; Mo, Y.; Liu, A.; Zhou, Z.; Tsai, K. R. *Inorg. Chem.* **2004**, *43*, 923–930.
(40) Zhou, T.; Mo, Y.; Zhou, Z.; Tsai, K. *Inorg. Chem.* **2005**, *44*, 4941–4946.
(41) Zampella, G.; Greco, C.; Fantucci, P.; De Gioia, L. *Inorg. Chem.* **2006**, *45*, 4109–4118.
(42) Becke, A. D. *J. Chem. Phys.* **1993**, *98*, 5648–5652.
(43) Lee, C.; Yang, W.; Parr, R. G. *Phys. Rev.* **1988**, *37*, 785–789.
(44) Frisch, M. J.; Trucks, G. W.; Schlegel, H. B.; Scuseria, G. E.; Robb, M. A.; Cheeseman, J. R.; Montgomery, J. A., Jr.; Vreven, T.; Kudin, K. N.; Burant, J. C.; Millam, J. M.; Iyengar, S. S.; Tomasi, J.; Barone, V.; Mennucci, B.; Cossi, M.; Scalmani, G.; Rega, N.; Petersson, G. A.; Nakatsuji, H.; Hada, M.; Ehara, M.; Toyota, K.; Fukuda, R.; Hasegawa, J.; Ishida, M.; Nakajima, T.; Honda, Y.; Kitao, O.; Nakai, H.; Klene, M.; Li, X.; Knox, J. E.; Hratchian, H. P.; Cross, J. B.; Bakken, V.; Adamo, C.; Jaramillo, J.; Gomperts, R.; Stratmann, R. E.; Yazyev, O.; Austin, A. J.; Cammi, R.; Pomelli, C.; Ochterski, J. W.; Ayala, P. Y.; Morokuma, K.; Voth, G. A.; Salvador, P.; Dannenberg, J. J.; Zakrzewski, V. G.; Dapprich, S.; Daniels, A. D.; Strain, M. C.; Farkas, O.; Malick, D. K.; Rabuck, A. D.; Raghavachari, K.; Foresman, J. B.; Ortiz, J. V.; Cui, Q.; Baboul, A. G.; Clifford, S.; Cioslowski, J.; Stefanov, B. B.; Liu, G.; Liashenko, A.; Piskorz, P.; Komaromi, I.; Martin, R. L.; Fox, D. J.; Keith, T.; Al-Laham, M. A.; Peng, C. Y.; Nanayakkara, A.; Challacombe, M.; Gill, P. M. W.; Johnson, B.; Chen, W.; Wong, M. W.; Gonzalez, C.; Pople, J. A. *Gaussian 03*, revision B.05; Gaussian, Inc.; Wallingford, CT, 2004.
(45) Hay, P. J.; Wadt, W. R. *J. Chem. Phys.* **1985**, *82*, 284–298.
(46) Hay, P. J.; Wadt, W. R. *J. Chem. Phys.* **1985**, *82*, 270–283.
(47) Couty, M.; Hall, M. B. *J. Comput. Chem.* **1996**, *17*, 1359–1370.
(48) Ehlers, A. W.; Böhme, M.; Dapprich, S.; Gobbi, A.; Höllwarth, A.; Jonas, V.; Köhler, K. F.; Stegmann, R.; Veldkamp, A.; Veldkamp, A.; Frenking, G. *Chem. Phys. Lett.* **1993**, *208*, 111–114.
(49) Höllwarth, A.; Böhme, M.; Dapprich, S.; Ehlers, A. W.; Gobbi, A.; Jonas, V.; Köhler, K. F.; Stegmann, R.; Veldkamp, A.; Frenking, G. *Chem. Phys. Lett.* **1993**, *208*, 237–240.
(50) Hariharan, P. C.; Pople, J. A. *Theor. Chim. Acta* **1973**, *28*, 213–222.
(51) Petersson, G. A.; Al-Laham, M. A. *J. Chem. Phys.* **1991**, *94*, 6081–6090.
(52) Petersson, G. A.; Bennett, A.; Tensfeldt, T. G.; Al-Laham, M. A.; Shirley, W. A.; Mantzaris, J. *J. Chem. Phys.* **1988**, *89*, 2193–2218.
(53) Hehre, W. J.; Ditchfield, R.; Pople, J. A. *J. Chem. Phys.* **1972**, *56*, 2257.
(54) Nakamoto, K. *IR and Raman Spectra of Inorganic and Coordination Compounds*, 5th ed.; Wiley-Interscience: New York, 1997; Parts A and B.

**Table 1.** Experimentally Determined $\nu$(CO) and $\nu$(CN) Bands for [FeFe]H$_2$ase Enzymes

| enzyme | state | $\nu$ (CO) | $\nu$ (CO) | $\nu$ (CO) | $\nu$ (CO) | $\nu$ (CX)[a] | $\nu$ (CN) | $\nu$ (CN) | ref |
|---|---|---|---|---|---|---|---|---|---|
| DdH/Dv | $H_{as\text{-}isolated}$[b] | | 2007 | 1983 | 1847 | | 2107 | 2087 | 18, 26 |
| DdH/Dv | $H_{ox}$[c] | | 1965 | 1940 | 1802 | | 2093 | 2079 | 18, 27 |
| DdH | $H_{ox}-{}^{13}CO$[d] | 1995 | 1963 | 1949 | 1812 | | 2096 | 2089 | 27 |
| DdH | $H_{ox}-{}^{12}CO$[e] | 2016 | 1972 | 1963 | 1811 | | 2096 | 2089 | 26, 27 |
| CpI | Hox[f] | | 1971 | 1948 | 1802 | | 2086 | 2072 | 28 |
| CpI | $H_{ox}-{}^{13}CO$[d] | 2000 | 1971 | 1947 | 1810 | | 2095 | 2077 | 28 |
| CpI | $H_{ox}-{}^{12}CO$[e] | 2017 | 1974 | 1971 | 1810 | | 2095 | 2077 | 28 |
| DdH/Dv | $H_{red}$[g] | 1965 | 1940 | 1916 | 1894 | 2041 | 2093 | 2079 | 18, 26 |

[a] X = O or N. [b] As isolated, in air [c] After electrochemical reduction at −535 mV, then oxidation at −285 mV or after reduction with $H_2$, then oxidation by $H_2$ loss under argon. [d] After reactivation with $H_2$, followed by $^{13}CO$ atmosphere. [e] After reactivation with $H_2$, followed by $^{12}CO$ atmosphere. [f] After reduction with $H_2$, then oxidation by $H_2$ loss under argon. [g] After electrochemical reduction at −535 mV or reduction with $H_2$.

tend to systematically overestimate the values of IR stretching frequencies when compared to experiment.[55] In order to predict $\nu_{CO}$ values from our computed stretching frequencies for the enzyme active site, a series of 15 iron−carbonyl complexes of similar composition to the [FeFe]H$_2$ase active site, were geometry optimized and their $\nu_{CO}$ stretching frequencies were computed. (The chemical structures and literature references for these complexes are given as Figure SI-1 and Table SI-1 in the Supporting Information.) The computed $\nu_{CO}$ and $\nu_{CN}$ values reproduce the $\nu_{CO}$ values of the experimental spectra well when multiplied by 0.9538 (i.e., $\nu_{CO}$(predicted) = 0.9538$\nu_{CO}$(computed)). The experimentally determined $\nu$(CO) values are plotted against the calculated $\nu$(CO) and $\nu$(CN) values in Figure SI-2. These complexes have total charges varying from 2+ to 2− and formal oxidation states of $Fe^{I}Fe^{I}$ and $Fe^{II}Fe^{II}$ for the iron centers. This large set of diverse complexes should minimize potential bias from the total charge and/or iron oxidation state on the predicted $\nu$(CO) stretching frequencies.[56] Corrected frequencies are used throughout this paper.

For terminal CO ligands, the experimentally determined $\nu$(CO) stretching frequencies are reproduced remarkably well by simple scaling of the computed $\nu$(CO) stretching frequencies. For bridging CO ligands, however, the predictions are more difficult. For example, the $[(\mu\text{-CO})(\mu\text{-S(CH}_2)_2\text{S})[\text{Fe(CNMe)}_3]_2]^{2+}$ and $[(\mu\text{-CO})(\mu\text{-S(CH}_2)_3\text{S})[\text{Fe(CNMe)}_3]_2]^{2+}$ complexes have been experimentally shown to have a $\nu$(CO) stretching frequency of 1914 cm$^{-1}$ and Fe−Fe distances of ∼2.5 Å.[57] Full geometry optimization of these complexes leads to predicted $\nu$(CO) stretching frequencies of 1960 and 1985 cm$^{-1}$ and Fe−Fe distances of 2.57 and 2.65 Å, respectively. Partial geometry optimization of these complexes with the Fe−Fe distance frozen at the experimentally determined distances of ∼2.5 Å led to predicted $\nu$(CO) stretching frequencies of 1949 and 1951 cm$^{-1}$, respectively. The predicted $\nu$(CN) stretching frequencies of the terminal CNMe ligands are very similar to the experimentally determined $\nu$(CN) stretching frequencies and are essentially unaffected by this small change in the Fe−Fe distance. The improved Fe−Fe distance brought the frequencies to the same value, but the value of the bridging CO band is still a little too high. Unfortunately, the test set based on known model compounds does not have any bridging CO ligands. Other functionals and basis sets need to be tested in the future to determine if a better Fe−Fe distance and improved $\nu$(CO) frequencies can be achieved.[58,59]

**Assignment of the Forms of the H-Cluster via Predicted IR Spectra. Assignment of the $H_{red}$ Form.** The $H_{red}$ form of the di-iron active site is the most reduced of the experimentally produced and spectroscopically observed forms of [FeFe]H$_2$ase, as evidenced by the relatively low $\nu$(CO) and $\nu$(CN) values observed for the terminal CO and $CN^-$ ligands. For the [FeFe]H$_2$ase enzyme derived from DdH/Dv, $H_{red}$ may be prepared by either electrochemical or chemical (incubation with $H_2$) reduction of the $H_{ox}^{air}$ form.[18,27]

Since there are more than three $\nu$(CO) bands present in the experimentally determined IR spectrum of the $H_{red}$ form of the [FeFe]H$_2$ase derived from DdH/Dv, this sample must contain a mixture of at least two different forms of the [FeFe]H$_2$ase active site. It is unclear if this spectrum represents two species that are more highly reduced than $H_{ox}$ or a mixture of $H_{ox}$ and one more highly reduced species. Infrared spectra of $H_{ox}$ show $\nu$(CN) bands at 2093 and 2079 cm$^{-1}$ and $\nu$(CO) bands at 1965, 1940, and 1802 cm$^{-1}$. Infrared spectra of the $H_{red}$ show $\nu$(CN) bands at 2093 and 2079 cm$^{-1}$, $\nu$(CO) bands at 1965, 1940, 1916, and 1894 cm$^{-1}$, and a $\nu$(CN) or $\nu$(CO) band at 2041 cm$^{-1}$. The true infrared spectrum for $H_{red}$ therefore may correspond to a reduced form with $\nu$(CN) bands at 2093 and 2079 cm$^{-1}$ and $\nu$(CO) bands at 2041, 1916, and 1894 cm$^{-1}$. One oddity of the $H_{red}$ spectrum is the large intensity of the $\nu$(CO) band at 1894 cm$^{-1}$ relative to the other $\nu$(CO) bands. In our models, the relative intensity of the 1894 band is explained by the overlap of either two or three $\nu$(CO) bands (vide supra). We were unable to determine any single structural candidates that reproduced the energies and relative intensities of the 2093, 2079, 2041, 1916, and 1894 cm$^{-1}$ bands (vide supra).

A series of highly reduced structural candidates were considered for the $H_{red}$ form (shown in Figure 2). Complexes **1**−**3** correspond to the $Fe^{I}Fe^{I}$ formal oxidation state, and complexes **4** and **5** correspond to hydrides with the $Fe^{II}Fe^{II}$

(55) Scott, A. P.; Radom, L. *J. Phys. Chem.* **1996**, *100*, 16502–16513.
(56) Tye, J. W.; Darensbourg, M. Y.; Hall, M. B. *J. Comput. Chem.* **2006**, *27*, 1454–1462.
(57) Boyke, C. A.; Rauchfuss, T. B.; Wilson, S. R.; Rohmer, M.-M.; Benard, M. *J. Am. Chem. Soc.* **2004**, *126*, 15151–15160.
(58) Silaghi-Dumitrescu, I.; Bitterwolf, T. E.; King, R. B. *J. Am. Chem. Soc.* **2006**, *128*, 5342–5343.
(59) Zilberman, S.; Stiefel, E. I.; Cohen, M. H.; Car, R. *Inorg. Chem.* **2006**, *45*, 5715–5717.

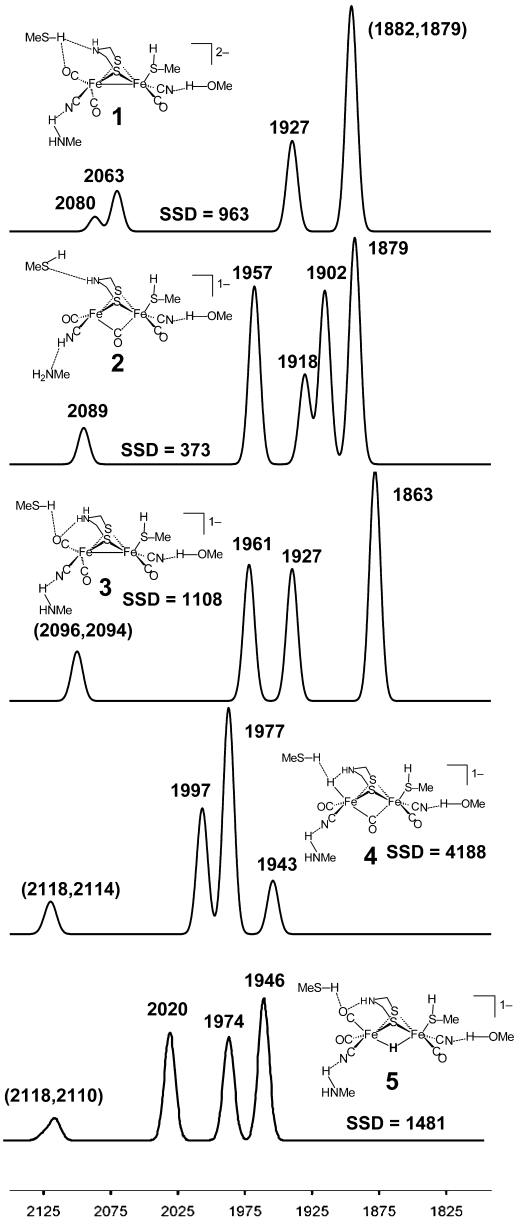


**Figure 2.** Predicted infrared spectra for various structural candidates for the $H_{red}$ form of the [FeFe]$H_2$ase enzyme derived from DdH (species **1**–**5**). All computed frequencies are scaled. SSD is the sum of the squares of the differences between the experimental and calculated spectra.

formal oxidation state.[60] Complexes **1**−**3** feature an open site on the distal iron center. The monoanionic complexes **2**−**5** are formally generated by protonation of the dianionic complex **1**. The additional $H^+$ is bound to the nitrogen of the distal cyanide ligand in complex **2** and to the amine nitrogen of the S-to-S linker in complex **3**. In complexes **4** and **5**, the additional $H^+$ is bound to the distal and both iron center(s) to yield terminal and bridging $Fe^{II}Fe^{II}$ hydride complexes, respectively.

The experimentally determined IR spectrum of the $H_{red}$ form of the [FeFe]$H_2$ase enzyme derived from DdH (Figure 3) can be compared to the predicted spectra for four structural candidates for the $H_{red}$ form in Figure 2. In terms of their predicted stretching frequencies and relative intensities of the $\nu$(CO) bands, the **1, 2**, and **5** species (Figure 2) are the best models for components present in the experimental spectra of the $H_{red}$ form. The sum of the squares of the differences (SSD's) between the experimentally determined and computed frequencies are given on each computed spectrum. In terms of the terminal CO bands, **3** is a good match to the 1965 and 1940 $cm^{-1}$ bands of the [FeFe]$H_2$ase enzyme derived from DdH (Figure 3). Species **4** is the least likely since the predicted $\nu$(CO) frequencies (Figure 2) for its terminal CO ligands fall in the blank region between 2041 and 1965 $cm^{-1}$ in the experimentally determined IR spectrum.

Several other structures were eliminated as structural candidates for the $H_{red}$ form (for structures and predicted IR spectra, see Figure SI-3 in the Supporting Information). For example, the addition of a water molecule near the distal iron center of **1** did not lead to an Fe−O bond following optimization, and this species has a predicted IR spectrum that is very similar to **1**. In other examples, the addition of a second proton to complex **2** or **4**, respectively, to yield an $Fe^{II}Fe^{II}$ complex with both a CNH ligand and a hydride ligand or an $Fe^{II}Fe^{II}$ $\eta^2$-$H_2$ complex led to predicted $\nu$(CO) and $\nu$(CN) stretching frequencies that were systematically too high when compared to experiment.

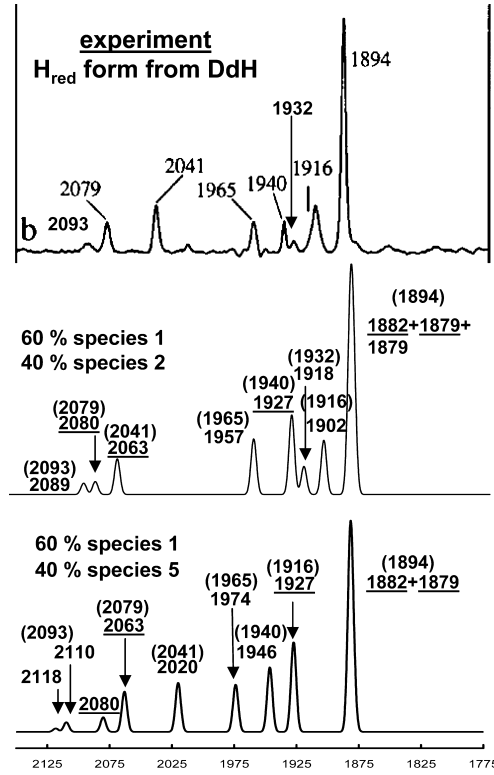


**Figure 3.** Experimentally determined infrared spectrum for the $H_{red}$ form of the [FeFe]$H_2$ase enzyme derived from DdH (top, reproduced from ref 18. 2001 American Chemical Society), predicted infrared spectra for a mixture of 60% of species **1** and 40% of species **2** (middle), and a mixture of 60% of species **1** and 40% of species **5** (bottom). All computed frequencies are scaled. The bands arising from complex **1** are underlined. The assigned bands from the experimental spectrum are given in parentheses.

(60) The hydrogen atom of the bridgehead amine can be oriented either toward the distal iron center or away from it. In general, the orientation of this hydrogen has little effect on the predicted IR spectra, and in all of the cases presented in this text, the orientation of hydrogen indicated gives as good or better qualitative agreement with the experimentally determined IR spectrum than the other orientation.

Figure 3 shows the predicted IR spectra for 40% **1**/60% **2**and 40% **1**/60% **5**. The predicted IR spectra arising from these mixtures are good qualitative matches for the experimentally determined IR spectrum of the $H_{red}$ form. Predicted IR spectra from "mixing" **1** and **3** or **2** and **3** resulted in IR spectra in which one or more of the weaker terminal $\nu$(CO) bands was too strong when compared to experiment. Depending on how one assigns the $\nu$(CO) and $\nu$(CN) bands, mixtures of of species **1** and **2** or **1** and **5** are equally good matches to the $H_{red}$ form.

**Assignment of the $H_{ox}$ Form.** For the di-iron active site, the $H_{ox}$ form is one-electron oxidized with respect to the $H_{red}$ form and one-electron reduced with respect to the $H_{ox}^{air}$ form, as evidenced the intermediacy of its terminal $\nu$(CO) and $\nu$(CN) values between those of the $H_{red}$ and $H_{ox}^{air}$ forms. EPR spectroscopy shows that the $H_{ox}$ form is an EPR-active, $S = {}^1/_2$ system. EPR and Mössbauer studies suggest that the unpaired electron is localized on the distal iron center.[20,21] The $H_{ox}$ form is generated by reduction of the $H_{ox}^{air}$ form to yield the $H_{red}$ form, followed by anerobic (chemical, auto-oxidation by $H_2$ loss under Ar, or electrochemical) oxidation of the $H_{red}$ form to yield the $H_{ox}$ form.[18,27]

A series of odd-electron ($S = {}^1/_2$), formally $Fe^IFe^{II}$ complexes were considered as structural candidates for the $H_{ox}$ form (shown in Figure 4). These complexes differ in the protonation state of the bridging amine and in the presence or absence of an additional ligand near the distal iron center. Complexes **6** and **7** feature a water molecule, complex **8** has an open site on the distal iron, and complex **9** has an $\eta^2$-$H_2$ ligand bound to the distal iron center. Complex **7** has an additional proton on the central nitrogen of the bridging dithiolate when compared to **6**. Geometry optimization of complexes **6** and **7**, which have a water molecule near the distal iron center, yielded Fe−O distances of 3.3 and 2.6 Å, respectively, between the distal iron center and the oxygen of this water molecule.

The experimentally determined IR spectrum of the $H_{ox}$ form of the [FeFe]$H_2$ase enzyme derived from DdH is compared to the predicted spectra for four structural candidates of the $H_{ox}$ form in Figure 4. In terms of their predicted stretching frequencies and relative intensities of the terminal $\nu$(CO) bands, all four of the structural candidates (complexes **6**−**9**) are similar to one another and a fairly good match to the experimental spectrum.

EPR and Mössbauer experiments suggest that the $H_{ox}$ form corresponds to a mixed valent $Fe^IFe^{II}$ form in which the unpaired electron is localized on the distal iron.[20,21] Fiedler and Brunold use computed EPR parameters for a large computational model of the [FeFe]$H_2$ase active site to assign the $H_{ox}$ form as a valence-localized $Fe^IFe^{II}$ form in which unpaired spin density is localized on the distal iron.[33] In terms of unpaired spin density, the complex with no ligand bound to the distal iron center, **8**, is the only good model for the $H_{ox}$ form in this sense, because, ∼90% of the computed Mulliken unpaired spin density (∼1 unpaired electron) lies on the distal iron center. The coordination of either $H_2O$ or $H_2$ to the distal iron center leads to a decrease of unpaired electron density on the distal iron center and an increase of unpaired electron density on the proximal iron center. Thus **6**, **7**, and **9** are all poor models for the $H_{ox}$ form of the active site, because the computed Mulliken spin density is distributed equally over the two iron centers. Nicolet et al. assign the $\nu$(CO) stretching frequencies observed for the $H_{ox}$ form of the [FeFe]$H_2$ase enzyme derived form DdH to the individual CO ligands of the [FeFe]$H_2$ase active site as shown in Figure 5. [18] Our predicted $\nu$(CO) spectra support their assignment. For **8**, the lowest and highest energy $\nu$(CO) bands (1802 and 1965 $cm^{-1}$ for DdH) arise primarily from the bridging CO ligand (CO(b) in Figure 5) and the terminal CO ligand coordinated to the proximal iron center (CO(a) in Figure 5). The intermediate $\nu$(CO) band (1940 $cm^{-1}$ for DdH) arises from the terminal CO ligand coordinated to the distal iron center (CO(c) in Figure 5).

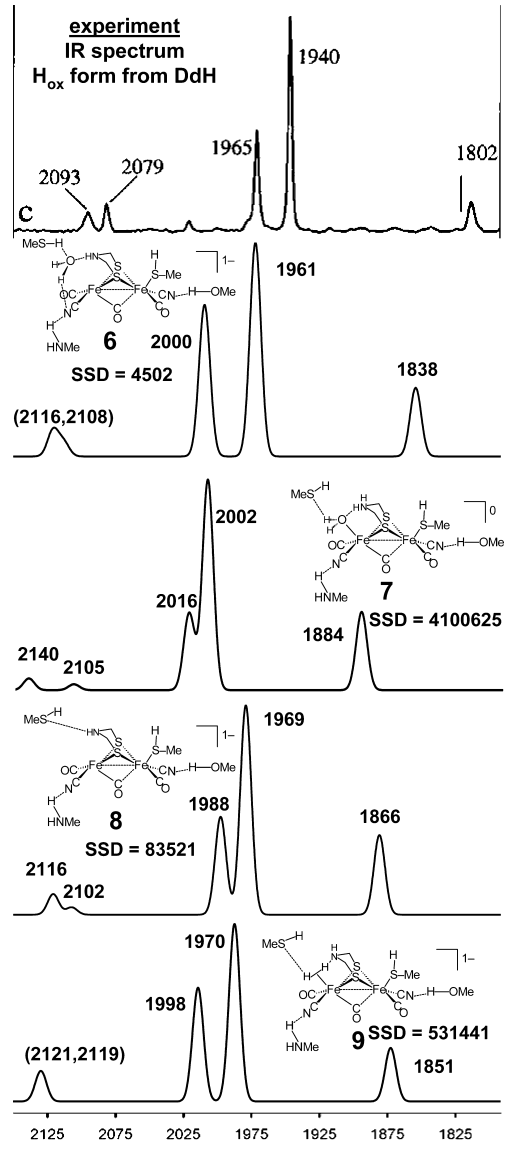


**Figure 4.** Experimentally determined infrared spectrum for the $H_{ox}$ form of the [FeFe]$H_2$ase enzyme derived from DdH (top, reproduced from ref 18. 2001 American Chemical Society) and predicted infrared spectra for various structural candidates for this form (species **6**–**9**). All computed frequencies are scaled. SSD is the sum of the squares of the differences between the experimental and calculated spectra.

**Assignment of the $H_{ox}$−CO Form.** The addition of CO gas to solutions of the catalytically active $H_{ox}$ form of the

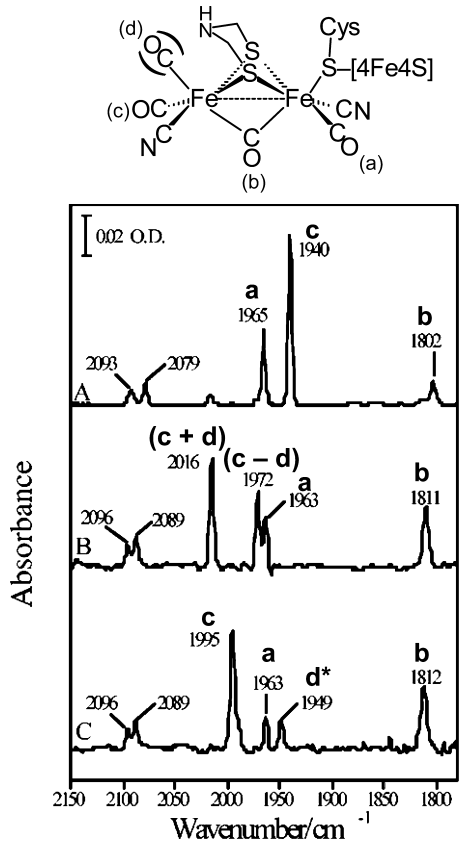


**Figure 5.** Experimentally determined infrared spectra from the $H_{ox}$ (A), $H_{ox}-{}^{12}CO$ (B), and $H_{ox}-{}^{13}CO$ (C) forms of [FeFe]$H_2$ase derived from DdH (reprinted from ref 28. 2000 American Chemical Society) with assignment of the $\nu$(CO) bands to the individual CO oscillators as suggested by De Lacey et al.

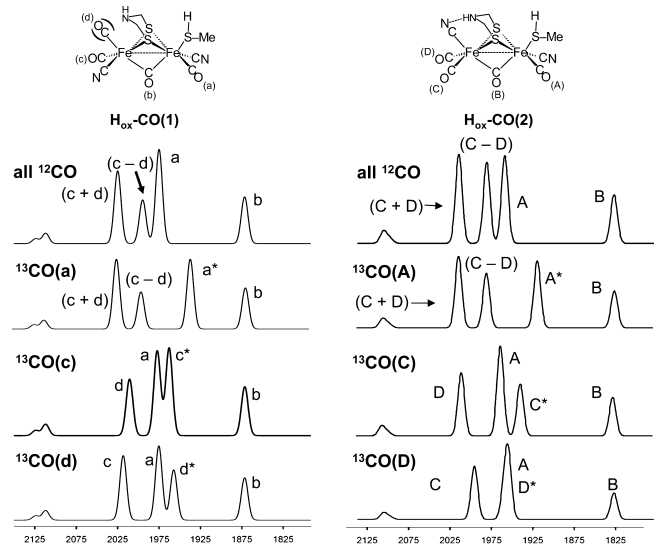


**Figure 6.** Predicted infrared spectra for computational models of two different proposed structural isomers of the $H_{ox}-CO$ form of the active site of [FeFe]$H_2$ase and various isotopomers of the $H_{ox}-{}^{13}CO$ form using the B3LYP functional. All computed frequencies are scaled. MeSH, $MeNH_2$, and MeOH models of the surrounding protein are included in the computation but omitted from the graphic above for clarity.

[FeFe]$H_2$ase enzyme leads to shifts in the $\nu$(CO) bands, the appearance of a new $\nu$(CO) band, and complete inhibition of catalytic $H_2$ oxidation and/or $H^+$ reduction.[16,28] The molecular structure derived from single crystal X-ray diffraction studies of the CO-inhibited form of the enzyme from CpI shows an additional CO ligand terminally coordinated to the distal iron center.[16] These results, taken together, suggest that CO inhibits the enzyme's catalytic activity by blocking the $H_2/H^+$ binding site on the distal iron center.

Direct evidence for location of the exogenous CO binding site comes from the comparison of the $H_{ox}$, $H_{ox}-{}^{12}CO$, and $H_{ox}-{}^{13}CO$ forms of the enzyme. The $H_{ox}-{}^{12}CO$ and $H_{ox}-{}^{13}CO$ designation indicates whether the [FeFe]$H_2$ase enzyme was exposed to natural abundance CO gas (mostly $^{12}CO$), or $^{13}CO$-enriched CO gas. De Lacey et al. and Nicolet et al. assign the $\nu$(CO) bands of the $H_{ox}$ and $H_{ox}-CO$ forms of the [FeFe]$H_2$ase enzyme derived from DdH as shown in Figure 5.[18,28] Chen et al. obtain similar results and make analogous assignments of the $\nu$(CO) bands for the $H_{ox}$, $H_{ox}-{}^{13}CO$, and $H_{ox}-{}^{12}CO$ forms of the [FeFe]$H_2$ase enzyme derived from CpI.[29]

Recently, Zilberman et al. used DFT-derived simulated IR spectra of computational models of the $^{12}CO-$ and $^{13}CO-H_{ox}$ forms to re-examine the structure of the $H_{ox}-CO$ form of [FeFe]$H_2$ase.[59] On the basis of calculations on [($\mu$-CO)($\mu$-$SCH_2XCH_2S$)[$Fe(CO)_2(CN)$][Fe(CO)(CN)($CH_3S$)]]$^{2-}$ (X = $CH_2$ and NH) with the PBE functional, they suggest a orientation of the CO and $CN^-$ ligands about the distal iron center (see right side of Figure 6) different than that originally proposed by Nicolet et al.,[18] De Lacey et al.,[28] and Chen et al.[29] Zilberman et al. suggest that exogenous CO binding to the distal iron center does not involve direct binding of CO to the apparent open site $H_{ox}$ form but, instead, a reorganization of the CO and CN ligands about that iron center precedes exogenous CO binding.

Predicted spectra for computational models of both of these proposed structural forms (labeled **$H_{ox}-CO(1)$** and **$H_{ox}-CO(2)$**) of the $H_{ox}-{}^{12}CO$ form of [FeFe]$H_2$ase are given in Figure 6. When compared to the experimentally determined IR spectrum of $H_{ox}-{}^{12}CO$ form of [FeFe]$H_2$ase enzyme derived from DdH (given in Figure 5), it is seen that although the relative intensities of the $\nu$(CO) bands are not perfectly reproduced by either model, the general pattern and the predicted values of the stretching frequencies of both models match well.

Comparison of the experimentally determined IR spectra for the $H_{ox}-{}^{12}CO$ and $H_{ox}-{}^{13}CO$ forms yields additional information about the exogenous CO binding site.[16,28] In the experimental studies of [FeFe]$H_2$ase enzyme derived from DdH, the 1963 and 1811/1812 $cm^{-1}$ bands are unchanged whether $^{12}CO$ or $^{13}CO$ gas is used to generate $H_{ox}-CO$. However, the other two $\nu$(CO) bands change depending on whether $^{12}CO$ or $^{13}CO$ gas is used to generate the $H_{ox}-CO$ form. These two $\nu$(CO) bands are observed at 2016 and 1972 $cm^{-1}$ for $H_{ox}-{}^{12}CO$ and at 1995 and 1949 $cm^{-1}$ for $H_{ox}-{}^{13}CO$.

The predicted IR spectra of three candidates for **$H_{ox}-{}^{13}CO(1)$**, isotopomers that only differ in the site of the $^{13}CO$ and the predicted IR spectrum of **$H_{ox}-{}^{12}CO(1)$** are presented in the left side of Figure 6. These calculations predict that the substitution of $^{12}CO$(a) by $^{13}CO$ should shift the band predicted at 1966 $cm^{-1}$ for **$H_{ox}-{}^{12}CO(1)$** to 1925

cm$^{-1}$ for **H$_{ox}$−$^{13}$CO(1)**. The substitution of the bridging CO ligand, CO(b), by $^{13}$CO leads to comparable shift to lower wave numbers (ca. −40 cm$^{-1}$) for the "1811/1812" cm$^{-1}$ band (spectra not shown). These low energy IR bands predicted for $^{13}$CO(a) and $^{13}$CO(b) substituted forms are not observed in the experimentally determined spectra of H$_{ox}$−$^{13}$CO. Therefore, exogenous $^{13}$CO is not binding in the CO(a) or CO(b) locations. The $^{13}$CO(c) and $^{13}$CO(d) substituted forms match the changes observed experimentally between the H$_{ox}$−$^{12}$CO and H$_{ox}$−$^{13}$CO forms. For these two isotopomers, the "1963" and 1811/1812 bands are virtually unshifted, while the remaining bands shift in a manner analogous to that observed in the experimental spectra. Therefore, the exogenous CO ligand must be either CO(c) or CO(d) or a mixture of CO(c) and CO(d). The results for the **H$_{ox}$−CO(2)** structural isomer are similar. The predicted IR spectra for **H$_{ox}$−$^{12}$CO(2)** are presented in the right side of Figure 6. These calculations predict that the substitution of $^{12}$CO(A) or $^{12}$CO(B) of **H$_{ox}$−CO(2)** by $^{13}$CO leads to a shift of those bands to lower wavenumbers (ca. −40 cm$^{-1}$). Therefore, the $^{13}$CO(c) and $^{13}$CO(d) substituted forms of **H$_{ox}$−CO(2)** also match the changes observed experimentally between the H$_{ox}$−$^{12}$CO and H$_{ox}$−$^{13}$CO forms.

In conclusion, in comparing the H$_{ox}$−$^{12}$CO and H$_{ox}$−$^{13}$CO forms, our computations using the B3LYP density functional show that either isomeric structure of the H$_{ox}$−CO form will yield qualitatively similar IR spectral results. The work of Zilberman et al. used unscaled frequencies the PBE density functional. As shown in Figure SI-4 in the Supporting Information, the use of the scaled B3LYP or unscaled PBE frequencies gave similar results for our extended computational model. Therefore, these computations do not discriminate between the two structural forms for the H$_{ox}$−CO form. Regardless of the precise structure, these computation agree that exogenous CO does not bind to the proximal iron or between the two irons. The lack of incorporation of $^{13}$CO into the bridging CO position suggests that exogenous CO cannot bind in this position. These results suggest that the $\mu$-CO forms of the [FeFe]H$_2$ase active site are not in equilibrium with forms that have all terminal CO ligands and provide strong evidence that the H$^+$/H$_2$ binding site is not located between the two iron centers.

**Assignment of the H$_{ox}^{air}$ Form.** The H$_{ox}^{air}$ form of the diiron active site is the most highly oxidized of the spectroscopically observed forms of the [FeFe]H$_2$ase enzyme, as evidenced by its high $\nu$(CO) and $\nu$(CN) values when compared to the other forms of the enzyme. The H$_{ox}^{air}$ form is an overoxidized, catalytically inactive form that results from aerobic purification of the enzyme from DdH/Dv. The H$_{ox}^{air}$ form may be reactivated by either chemical or electrochemical reduction.[18,27]

The experimentally determined IR spectrum of the catalytically inactive, EPR-silent, H$_{ox}^{air}$ form of the [FeFe]H$_2$ase enzyme derived from DdH is compared to the predicted spectra for three structural candidates of the H$_{ox}^{air}$ form in Figure 7. These candidates differ in the ligand coordinated to the distal iron center. Complexes **10**, **11**, and **12** feature hydroxy (OH−),

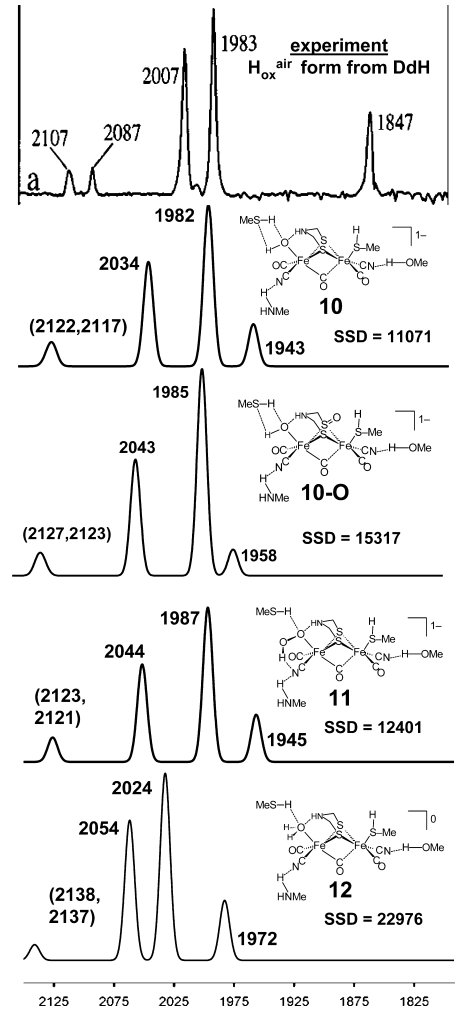


**Figure 7.** Experimentally determined infrared spectrum for the H$_{ox}^{air}$ form of the [FeFe]H$_2$ase enzyme derived from DdH (top, reproduced from ref 18. 2001 American Chemical Society) and predicted infrared spectra for various structural candidates for this form (species **10**−**12**). All computed frequencies are scaled. SSD is the sum of the squares of the differences between the experimental and calculated spectra.

hydroperoxy (OOH−), and water (H$_2$O), respectively, bound to the distal iron center. In terms of their predicted stretching frequencies and relative intensities of the $\nu$(CO) bands, species **10** and **11** are both good models for the species observed in the experimental IR spectrum of the H$_{ox}^{air}$ form of the active site of [FeFe]H$_2$ase. The pattern and relative intensities of the $\nu$(CO) bands in the predicted spectrum of **12** are a good match to the experimental IR spectrum, but the predicted frequencies of terminal CO bands are systematically too high.

Species **11**, which contains an OOH$^-$ ligand bound to the distal iron center, is a particularly appealing candidate for the structure of the H$_{ox}^{air}$ form of [FeFe]H$_2$ase for several reasons, in addition to its good agreement with the infrared spectrum. The overoxidized catalytically inactive H$_{ox}^{air}$ form is slowly reactivated by electrochemical or chemical reduction. Recent results suggest that this reactivation by reduction to the H$_{ox}$ form appears to require three electrons.[30] The need to remove a bound OOH$^-$ ligand by reduction to two molecules of H$_2$O, which was recently proposed for the reactivation of the catalytically inactive Ni−A form of [NiFe]H$_2$ase enzyme derived from *Desulfovibrio fructosovorans*,[61] could explain the three electrons

required for conversion of the $Fe^{II}Fe^{II}$ $H_{ox}^{air}$ form into the $Fe^{I}Fe^{II}$ $H_{ox}$ form.[30,61] The refinement of the crystal data obtained for the [FeFe]$H_2$ase enzyme derived from CpI (PDB ID's: 1FEH and 1C4A) yielded an oxygen atom at a distance of 2.55Å from the distal iron center, which was assigned as belonging to a water molecule bound to the distal iron site.[15,16] This iron−oxygen distance is quite long when compared to iron complexes that contain a terminally coordinated water molecule. A survey of the Cambridge Structural Database shows that iron−oxygen distances for synthetic iron(II) complexes of water range from 1.919 to 2.277 Å.[62,63] In particular, the [*trans*-$Fe(depe)_2(H_2O)(CO)]^{2+}$ complex was shown to have iron−oxygen distances of 2.036 and 2.051 Å in two separate solid-state structure determinations.[64] In addition, DFT geometry optimization of computational models of the $Fe^{II}Fe^{II}$ forms of the [FeFe]$H_2$ase active site with $H_2O$ or $OH^-$ ligands lead to iron−oxygen distances of ~2 Å. Fontecilla-Camps and coworkers recently showed that the overoxidized, catalytically inactive form (referred to as Ni−A) of a [NiFe]$H_2$ase enzyme derived from *Desulfovibrio fructosovorans,* whose X-ray structure was originally refined to show a bridging oxo or hydroxo bridge ($O^{2-}$ or $OH^-$), in fact contained a hydroperoxo ligand ($OOH^-$). These results, taken together, suggest that the $H_{ox}^{air}$form of the [FeFe]$H_2$ase enzyme derived from DdH may actually contain an $OOH^-$ ligand bound to the distal iron center.

Our recent computational work suggests that the Ni−A form of [NiFe]$H_2$ase enzyme may instead consist of a $OH^-$ bridged Ni−Fe cluster with an oxygen atom attached to the sulfur atom of one of the terminal thiolate ligands.[65] In this context, we evaluate possible alternative structures for the $H_{ox}^{air}$ form of [FeFe]$H_2$ase in which one of the sulfur atoms of the dithiolate linker has been oxidized. The predicted infrared spectra for the terminal $OH^-$ complex, **10**, and a complex similar to **10** with an oxygen atom bound to one of the bridging thiolate sulfur atoms, **10-O**, are given in Figure 7. Although the predicted $\nu$(CO) bands of **10** are shifted to slightly higher values in **10-O** (~5–10 $cm^{-1}$), the predicted spectra of **10** and **10-O** are very similar qualitatively. In addition, our results suggest that the sulfur-oxidized, $OH^-$ complex **10-O** could be obtained from the $OOH^-$ complex **11**. We calculate the transfer of one oxygen atom from a terminal, distal iron-bound $OOH^-$ ligand of **11** to one of the sulfur of the dithiolate linker to yield **10-O** to be exothermic by 21.7 kcal $mol^{-1}$. A similar type of complex has been observed experimentally in the reaction of ($\mu$-$SCH_2$-$CH_2S$)$[Fe(CO)_3]_2$ with *m*-chloroperbenzoic acid to yield the sulfoxy species, ($\mu$-$SCH_2CH_2S$=**O**)$[Fe(CO)_3]_2$.

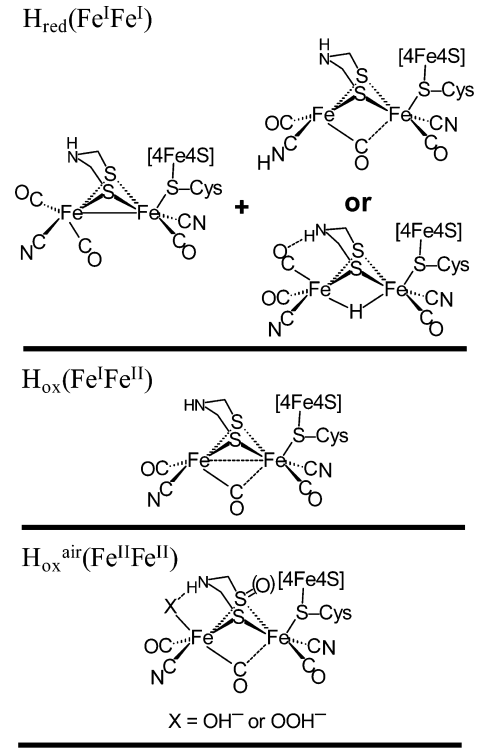


**Figure 8.** Best structural candidates for the $H_{red}$, $H_{ox}$, and $H_{ox}^{air}$ forms of [FeFe]$H_2$ase. The $H_{red}$ form is assigned as a mixture of two species. One of the bridging thiolate sulfur atoms may be oxidized in the $H_{ox}^{air}$ form. The formal oxidation states of the iron centers in each form is given in parentheses.

## Conclusions

On the basis of our computations, the best structural candidates for the $H_{red}$, $H_{ox}$, and $H_{ox}^{air}$ forms are as given in Figure 8. The $H_{red}$ form is assigned as a mixture of an $Fe^IFe^I$ form with an open site on the distal iron center and either a $Fe^IFe^I$ form in which the distal cyanide has been protonated or a $Fe^{II}Fe^{II}$ form with a bridging hydride ligand. The $H_{ox}$ form is assigned as a valence-localized $Fe^IFe^{II}$ redox level with no ligand bound at the distal iron. The $H_{ox}^{air}$ form is assigned as an $Fe^{II}Fe^{II}$ redox level with an $OH^-$ or $OOH^-$ bound to the distal iron center and may or may not have an oxygen atom bound to one of the sulfur atoms of the dithiolate linker.

**Acknowledgment.** We acknowledge financial support from the National Science Foundation (CHE-0616695 to M.Y.D., CHE-0518047 to M.B.H.) and R. A. Welch Foundation (A-0924 to M.Y.D. and A-0648 to M.B.H.). We also thank the Supercomputing Facility, the Tensor Beowulf cluster (NSF DMS-0216275), and the Laboratory for Molecular Simulation at Texas A&M University for computer time and software. We thank J. C. Fontecilla-Camps and D. J. Darensbourg for helpful discussions.

**Supporting Information Available:** Structures and literature references for the synthetic di-iron complexes used in the training set. Structures and simulated infrared spectra for additional structural candidates for the $H_{red}$ form. This material is available free of charge via the Internet at http://pubs.acs.org.

IC7013732

(61) Volbeda, A.; Martin, L.; Cavazza, C.; Matho, M.; Faber, B. W.; Roseboom, W.; Albracht, S. P. J.; Garcin, E.; Rousset, M.; Fontecilla-Camps, J. C. *JBIC, J. Biol. Inorg. Chem.* **2005**, *10*, 239–249.
(62) Bernal, I.; Jensen, I. M.; Jensen, K. B.; McKenzie, C. J.; Toftlund, H.; Tuchagues, J.-P. *Dalton Trans.* **1995**, *22*, 3667–3675.
(63) Laine, P.; Gourdon, A.; Launay, J.-P.; Tuchagues, J.-P. *Inorg. Chem.* **1995**, *34*, 5150–5155.
(64) Landau, S. E.; Morris, R. H.; Lough, A. J. *Inorg. Chem.* **1999**, *38*, 6060–6068.
(65) Pardo, A.; DeLacey, A. L.; Fernandez, V. M.; Fan, H.-J.; Fan, Y.; Hall, M. B. *JBIC, J. Biol. Inorg. Chem.* **2006**, *11*, 286–306.
(66) Messelhäuser, J.; Gutensohn, K. U.; Lorenz, I.-P.; Hiller, W. *J. Organomet. Chem.* **1987**, *321*, 377–388.